



Photoluminescence and scintillation properties of Ce-doped $\text{Sr}_2(\text{Gd}_{1-x}\text{Lu}_x)_8(\text{SiO}_4)_6\text{O}_2$ ($x = 0.1, 0.2, 0.4, 0.5, 0.6$) crystals

Takuya Igashira*, Naoki Kawano, Go Okada, Noriaki Kawaguchi, Takayuki Yanagida

Graduate School of Materials Science, Nara Institute of Science and Technology (NAIST), 8916-5, Takayama, Ikoma, Nara, Japan

ARTICLE INFO

Keywords:

Scintillator

Ce^{3+}

Apatite

Scintillation

ABSTRACT

Apatite crystals with chemical compositions of 0.5% Ce-doped $\text{Sr}_2(\text{Gd}_{1-x}\text{Lu}_x)_8(\text{SiO}_4)_6\text{O}_2$ ($x = 0.1, 0.2, 0.4, 0.5, 0.6$) were synthesized by the Floating Zone method, and then we evaluated their photoluminescence (PL) and scintillation properties. All the Ce-doped samples exhibited PL and scintillation with an intense broad emission in 400–550 nm in which the origin was attributed to the 5d–4f transition of Ce^{3+} , and the emission peak became broader with increasing the concentration of Lu^{3+} . Both PL and scintillation decay time profiles were best-approximated by a sum of two exponential decay functions, and the origin of slower component was attributed to the 5d–4f transition of Ce^{3+} . In the X-ray induced afterglow measurements, the Ce-doped $\text{Sr}_2(\text{Gd}_{0.4}\text{Lu}_{0.6})_8(\text{SiO}_4)_6\text{O}_2$ sample exhibited the lowest afterglow level. Furthermore, the Ce-doped $\text{Sr}_2(\text{Gd}_{0.5}\text{Lu}_{0.5})_8(\text{SiO}_4)_6\text{O}_2$ and $\text{Sr}_2(\text{Gd}_{0.4}\text{Lu}_{0.6})_8(\text{SiO}_4)_6\text{O}_2$ samples showed a clear full energy deposited peak under 5.5 MeV ^{241}Am α -ray irradiation, and the estimated absolute scintillation light yields were around 290 and 1300 ph/5.5 MeV- α , respectively.

1. Introduction

Inorganic scintillators are a type of phosphors that convert a single quantum of high energy (keV–GeV) radiation (e.g., α -, β -, X- and γ -rays) to a larger number of low energy photons (e.g., visible-ultraviolet light typically in 2–8 eV) [1]. Scintillators play an important role for ionizing radiation detectors used in a wide range of applications such as medical imaging [2], security system [3], well-logging [4], high energy physics [5], nuclear physics [6], astroparticle physics [7] and astrophysics [8]. Required characteristics of scintillators vary depending on the application; but, light yield, decay time and effective atomic number (Z_{eff}) [9,10] are typically considered. Most scintillators consist of a host material and dopant element which have functions to absorb the radiation energy to act as emission center, respectively. In terms of the dopant element, rare-earth elements (e.g., Ce^{3+} , Pr^{3+} , Nd^{3+} , Sm^{3+} , Eu^{2+} , Tb^{3+} , Dy^{3+} , Ho^{3+} , Er^{3+} and Tm^{3+}) have been particularly attracted [11–17]. Among such elements, Ce^{3+} exhibits bright luminescence with a short decay time (several tens of nanosecond) due to the parity- and spin-allowed 5d–4f transitions [1], and it has often been selected as emission center of many practical scintillators [18–20]. Moreover, the combination of Ce^{3+} -emission center and Gd-constituting host has a great attention as scintillator because (1) the ionic radii of Gd^{3+} and Ce^{3+} are well-matched so the Ce^{3+} ion can easily replace for the Gd^{3+} ion in the host and (2) energy transfer from the

Gd^{3+} to Ce^{3+} are often reported [21,22]. A past study has reported that Ce-doped Gd-based scintillator exhibited a high light yield up to 40,000–50,000 ph/MeV under γ -ray irradiation [20]. Although the performance of the above scintillators are acceptable for practical applications in general, scintillators with higher performance have been progressively desired for demanding and state-of-the-art applications.

Motivated by earlier studies, we have been investigating Ce-doped Gd-based apatite crystals which are represented as $\text{RE}_9\text{Si}_6\text{O}_{26}$ and $\text{AE}_2\text{RE}_8\text{Si}_6\text{O}_{26}$, where RE and AE denote rare-earth and alkaline-earth elements, respectively [23]. In general, apatite materials are applied in medicine as for artificial bone [24] and other applications [25,26]. In our previous research, we synthesized Ce-doped $\text{Sr}_2\text{Gd}_8(\text{SiO}_4)_6\text{O}_2$ crystals and evaluated the scintillation properties [27]. Although we observed a clear full-energy deposited peak under 5.5 MeV α -ray irradiation, the decay time was longer than those of commonly reported Ce-doped Gd-based scintillators. We concluded that the reason of longer decay time was due to energy migration processes from Gd^{3+} to Ce^{3+} . Hence, we replaced the Gd^{3+} ion by Lu^{3+} (i.e. Ce-doped $\text{Sr}_2\text{Lu}_8(\text{SiO}_4)_6\text{O}_2$) and then evaluated the scintillation properties [28]. As a result, we obtained not only faster decay time but also much higher absolute scintillation light yield (940 ph/5.5 MeV- α) than Gd-based apatite crystals. However, some impurity phases were confirmed in Ce-doped $\text{Sr}_2\text{Lu}_8(\text{SiO}_4)_6\text{O}_2$ sample by X-ray diffraction (XRD). We could not synthesize a bulk single crystal of Lu-based host material

* Corresponding author.

E-mail address: igashira.takuya.il4@ms.naist.jp (T. Igashira).

because the ionic radii of Lu^{3+} (host) and Ce^{3+} and Sr^{2+} (substitutes) were largely different to maintain the macroscopic structure. Nevertheless, there is still a large room for studying apatite scintillators, and one of the attracting investigations is to introduce both Gd^{3+} and Lu^{3+} ions together to the RE site with varying ratios.

In the present research, we synthesized 0.5% Ce-doped $\text{Sr}_2(\text{Gd}_{1-x}\text{Lu}_x)_8(\text{SiO}_4)_6\text{O}_2$ ($x = 0.1, 0.2, 0.4, 0.5, 0.6$) (hereafter Gd 90%, Gd 80%, Gd 60%, Gd 50% and Gd 40%, respectively) apatite crystals by the Floating Zone (FZ) method. In addition, we synthesized non-doped $\text{Sr}_2(\text{Gd}_{0.4}\text{Lu}_{0.6})_8(\text{SiO}_4)_6\text{O}_2$ for an aid to identify emission origins. Furthermore, we investigated their crystalline structures, photoluminescence (PL) and scintillation properties via characterizations of XRD, PL excitation and emission spectra, PL decay profiles, scintillation spectra, scintillation decay profiles, afterglow profiles and pulse height spectra under ^{241}Am α -ray irradiation.

2. Experimental procedures

0.5% Ce-doped Gd 90%, Gd 80%, Gd 60%, Gd 50% and Gd 40% apatite crystals ($(\text{Ce}_{0.005}\text{Gd}_{0.995-x}\text{Lu}_x)_8\text{Sr}_2(\text{SiO}_4)_6\text{O}_2$; $x = 0.1, 0.2, 0.4, 0.5, 0.6$) as well as non-doped Gd 40% apatite crystal ($(\text{Gd}_{0.4}\text{Lu}_{0.6})_8\text{Sr}_2(\text{SiO}_4)_6\text{O}_2$) were synthesized by the FZ method as follows. First, raw material powders of CeO_2 , Gd_2O_3 , Lu_2O_3 , SrCO_3 and SiO_2 were mixed by using mortar and pestle. Next, the mixture powder was heated at 1100°C for 10 h so as to remove CO_2 from SrCO_3 . Then, the obtained mixture powder was formed to a cylinder by loading the powder in a cylindrical balloon and then applying a hydrostatic pressure. The cylinder rod of powder mixture was sintered at 1500°C for 12 h to make into ceramic. Finally, the ceramic rod was loaded into an FZ furnace (FZD0192, Canon Machinery Inc.) to grow a crystal under ambient atmosphere. Here, the pull-down rate was approximately 5 mm/h, and the rotation rate was 20 rpm. Crystalline structures of the synthesized samples were identified by XRD using a diffractometer (MiniFlex600, Rigaku).

The PL excitation and emission spectra as well as PL quantum yield (QY) were measured by using Quantaaurus-QY (C11347, Hamamatsu). The measured spectral ranges of excitation and emission were 250–500 and 200–900 nm, respectively. The interval for the excitation wavelength was 10 nm. The PL QY was defined as: $\text{QY} (\%) = N_{\text{emit}}/N_{\text{absorb}}$ where N_{emit} and N_{absorb} are the numbers of emitted and absorbed photons, respectively. PL decay time profile was evaluated by Quantaaurus- τ (C11367, Hamamatsu). Here, the monitored emission wavelength was 425 nm, and the excitation wavelength was fixed to 340 nm. These optical measurements were done at room temperature.

The X-ray induced scintillation spectra were measured by using our original setup [29]. The excitation source used here was a conventional X-ray tube (XRBOP&N200X4550, Spellman) which was supplied with 80 kV bias voltage and 1.2 mA tube current by X-ray generator. The scintillation photons from the sample was fed into an optical fiber to guide to a monochromator (SR163, ANDOR) which is equipped with a charge coupled device (CCD) detector (DU920-BU2NC, ANDOR). The scintillation decay time profile and X-ray induced afterglow profile were measured by using our original setup, which is equipped with a pulse X-ray tube [30]. Here, the applied tube voltage was 30 kV, and the X-ray pulse width and repetition rate were a few ns and 200 kHz, respectively. The X-ray induced afterglow profiles were also evaluated by using the same setup but an X-ray pulse with of ms at 10 Hz. We evaluated the absolute scintillation light yield using pulse height spectroscopy technique under ^{241}Am α -rays. A sample was placed on a window of photomultiplier tube (PMT; R7600, Hamamatsu) with optical grease (OKEN6262A, OKEN), and then the sample was covered by layers of Teflon tape with a small hole punched for the α -rays to make it to the sample. During the measurement, a bias voltage of 700 V was supplied to the PMT by using a DC power supply (556, ORTEC). Moreover, the amplified signal was processed by a shaping amplifier (ORTEC572, ORTEC) with 1 μs shaping time. The signal output per

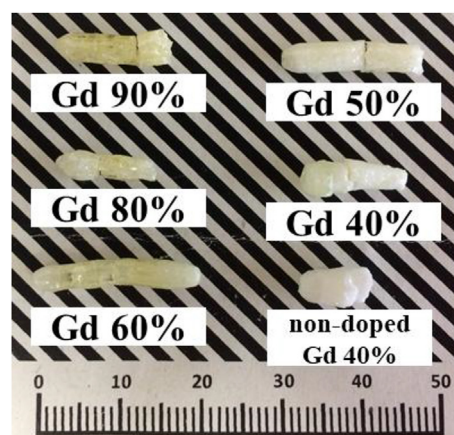


Fig. 1. Ce-doped and non-doped apatite crystals with different ratios Gd^{3+} to Lu^{3+} .

single event was statistically accumulated by a multichannel analyzer (MCA-8000A, Amptek) to construct a pulse height spectrum.

3. Results and discussion

3.1. Sample

Fig. 1 shows the synthesized Ce-doped apatite crystals with different ratios of Gd^{3+} to Lu^{3+} as well as non-doped Gd 40%. The typical sample size was approximately 3 mm in diameter and 10–20 mm in length. The color of the most Ce-doped samples was yellow which is typical for Ce-doped phosphors due to optical absorption by the 4f–5d transition of Ce^{3+} [31]. We also confirmed that the yellow color of samples disappeared with increasing the concentration of Lu^{3+} . Under UV lamp (302 nm), we observed blue PL emission due to the 5d–4f transition of Ce^{3+} by eye for all the samples. Measured powder XRD patterns of all the samples are illustrated in Fig. 2, together with the JCPDS standard pattern of $\text{Ca}_2\text{Gd}_8(\text{SiO}_4)_6\text{O}_2$ apatite single crystal (No: 28-0212) as a reference. We confirmed from the XRD patterns that all the samples have mainly the apatite phase. Regarding the samples with less than 40% of Gd^{3+} , the XRD patterns showed some impurity phases. In crystallography, we know that ionic radii of substituting and substituted elements should be sufficiently close in order to maintain the crystal structure. And, in our system, compared with the ionic radii of Ce^{3+} and Sr^{2+} , the ionic radius of Lu^{3+} is more largely different than Gd^{3+} . Therefore, we think that the samples with less than 40% of Gd^{3+} could not be grown in a single phase; thus, we stopped making samples at this composition. The obtained crystal rods were cut to a typical size of approximately 3 mm in diameter and 2 mm in thickness in order to evaluate the PL and scintillation properties.

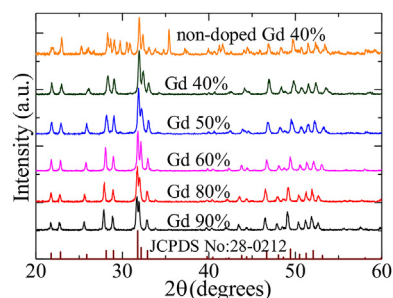


Fig. 2. XRD patterns of Ce-doped Gd 90%, Gd 80%, Gd 60%, Gd 50% and Gd 40% as well as non-doped Gd 40% samples.

Download English Version:

<https://daneshyari.com/en/article/7906669>

Download Persian Version:

<https://daneshyari.com/article/7906669>

[Daneshyari.com](https://daneshyari.com)